

## Wall tensions of model colloid–polymer mixtures

This article has been downloaded from IOPscience. Please scroll down to see the full text article.

2004 J. Phys.: Condens. Matter 16 L1

(<http://iopscience.iop.org/0953-8984/16/1/L01>)

View [the table of contents for this issue](#), or go to the [journal homepage](#) for more

Download details:

IP Address: 171.66.16.125

The article was downloaded on 19/05/2010 at 17:55

Please note that [terms and conditions apply](#).

## LETTER TO THE EDITOR

**Wall tensions of model colloid–polymer mixtures****Paul P F Wessels<sup>1</sup>, Matthias Schmidt<sup>2,3</sup> and Hartmut Löwen<sup>1</sup>**<sup>1</sup> Institut für Theoretische Physik II, Heinrich-Heine-Universität Düsseldorf, Universitätsstraße 1, 40225 Düsseldorf, Germany<sup>2</sup> Debye Institute, Utrecht University, Princetonplein 5, 3584 CC Utrecht, The Netherlands

Received 5 November 2003

Published 15 December 2003

Online at [stacks.iop.org/JPhysCM/16/L1](http://stacks.iop.org/JPhysCM/16/L1) (DOI: 10.1088/0953-8984/16/1/L01)**Abstract**

Using the Asakura–Oosawa–Vrij model for mixtures of hard sphere colloids and non-adsorbing polymer coils, an analytic formula for the interfacial free energy of the fluid mixture in contact with a hard wall is obtained within a scaled-particle treatment. The results compare well with explicit density functional calculations for the binary mixture. We also give expressions for the wall tension of the mixture when polymers interact via a simple stepfunction pair potential, and for the case of contact with a polymer-coated wall, which we take to be hard for the colloids but penetrable for the polymers. On the gas side of the fluid–fluid demixing binodal we confirm the wetting transition at the hard wall and predict complete drying of the polymer-coated wall on the liquid side of the binodal.

Mixtures of sterically-stabilized colloidal particles and non-adsorbing globular polymers suspended in an organic solvent are valuable soft matter systems to study demixing phase transitions and wetting phenomena at walls; for a recent review see [1]. Controlling the wetting behaviour is mandatory for tailoring wall coatings with intriguing applications like self-cleaning surfaces [2]. Experimental investigations of well-characterized model systems have provided direct insight into the bulk phase diagram [1], the fluid–fluid surface tension (i.e. the interfacial free energy between colloidal liquid and colloidal gas phases) [3–6], and the wetting behaviour of walls [6–9]. In order to capture the key features of the microscopic interactions, the Asakura–Oosawa–Vrij (AO) model [10, 11] of hard sphere colloids and ideal polymer spheres has become a widely-used reference system. Recently, studies based on density functional theory (DFT) [12–16] and computer simulations [17–19] have been performed in order to explore the bulk phase diagram [13, 17, 18] (validating the accuracy of the celebrated free-volume theory [20]), the wetting and layering behaviour at a hard wall [14, 15, 17, 21], the surface tension between colloidal liquid and gas phases [12, 14, 15, 19, 21, 22], and capillary condensation in a slit pore [16]. The basic features are in agreement with experimental results

<sup>3</sup> On leave from: Institut für Theoretische Physik II, Heinrich-Heine-Universität Düsseldorf, Universitätsstraße 1, 40225 Düsseldorf, Germany.

and some deviations in the fluid demixing binodal can be improved by approximating realistic polymer–polymer interactions [18] in a simple way [23]. The physical key quantities dictating wetting and drying behaviour at walls, when the bulk is at or near fluid–fluid coexistence, are the interface tensions between wall and liquid,  $\gamma_{wl}$ , and between wall and gas,  $\gamma_{wg}$ , as well as the surface tension of the (free) liquid–gas interface,  $\gamma_{lg}$ . Those enter directly into Young’s equation for the contact angle  $\theta$  at which the gas–liquid interface hits the wall [24],  $\gamma_{lg} \cos \theta = \gamma_{wg} - \gamma_{wl}$ . Despite the rapidly growing number of experimental [6–9] and theoretical [14, 15, 17, 21] papers on wetting phenomena of colloid–polymer mixtures, investigations of the tension of polymers at surfaces of colloidal particles [25], and geometrical analysis of depletion near walls [21], neither  $\gamma_{wg}$  and  $\gamma_{wl}$  nor the wall–fluid tension away from coexistence,  $\gamma_{wf}$ , have been addressed directly.

In this letter, we present an analytical expression for  $\gamma_{wf}$  of the AO model at a hard wall using ideas from scaled particle theory (SPT) originally developed in [26–30] and successfully tested [31, 32] for hard sphere mixtures. The key idea is to consider a *ternary* system of colloids, polymers and a dummy component of large size and vanishing concentration that is equivalent to a planar wall. The bulk free energy  $F$  of the ternary mixture is required as an input, and a systematic expansion allows us to determine  $\gamma_{wf}$ . Evaluating  $\gamma_{wf}$  at the gas (liquid) branch of the binodal yields an estimate for  $\gamma_{wg}$  ( $\gamma_{wl}$ ). We take  $F$  from (straightforward generalizations) of free-volume theory [20], and DFT [23], the latter including polymer–polymer interactions in a simple way. We find that polymer non-ideality significantly increases  $\gamma_{wf}$  compared to the case of ideal polymers at the same statepoint. We also consider the effect of polymer chains that are grafted to a substrate [9], and take this composite to exert a hard core repulsion on the colloids, but to be fully penetrable for the polymers. In all cases, analytical expressions for  $\gamma_{wf}$  are presented and found to compare well with the results from explicit DFT calculations for the binary AO model. Comparing  $\gamma_{wl} - \gamma_{wg}$  to DFT results for  $\gamma_{lg}$  allows us to confirm the wetting transition at the hard wall on the gas branch [14, 15], and to predict complete drying of the polymer-coated wall everywhere on the liquid branch of the fluid demixing binodal. Our results for  $\gamma_{wf}$  can be tested against those from computer simulations (see, for example, [19] for an investigation of  $\gamma_{lg}$  and comparison to DFT results). The wall tension that we are concerned with is that which solely arises due to the presence of the mesoscopic particles and the suspended polymer chains. In a real mixture, there will also be a strong contribution to the tension due to the molecular solvent; we guess that this makes measuring the osmotic contribution a challenge. To the best of our knowledge interfacial tensions of non-additive mixtures have not been considered before with SPT [33].

The theoretical model [10, 11, 23] consists of hard sphere colloids (species c) and polymer spheres (species p) with diameters  $\sigma_c$  and  $\sigma_p$  and particle numbers  $N_c$  and  $N_p$ , respectively, within a volume  $V$ . The particles interact via pairwise potentials given as a function of the centre–centre distance  $r$  as  $u_{cc}(r) = \infty$  if  $r < \sigma_c$  and zero otherwise,  $u_{cp}(r) = \infty$  if  $r < (\sigma_c + \sigma_p)/2$  and zero otherwise,  $u_{pp}(r) = \epsilon$  if  $r < \sigma_p$  and zero otherwise. Control parameters are the size ratio  $q = \sigma_p/\sigma_c$ , and a scaled energy,  $\beta\epsilon$ , where  $\beta = 1/(k_B T)$ ,  $k_B$  is the Boltzmann constant and  $T$  is the temperature. For  $\beta\epsilon = 0$  the polymers are ideal and we are dealing with the AO model; for  $\beta\epsilon \rightarrow \infty$  the binary hard sphere mixture is recovered. Two different cases for the dummy component (species d) are considered. In the first case of the hard wall, the dummy is similar to a (large) colloid, hence its interaction with species  $i = c, p$  is  $u_{di} = \infty$  if  $r < (\sigma_d + \sigma_i)/2$  and zero otherwise. In the second case of the polymer-coated wall the dummy behaves like a (large) polymer and hence interacts with colloids as  $u_{dc}(r) = \infty$  if  $r < (\sigma_d + \sigma_c)/2$  and zero otherwise; the interaction with polymers is  $u_{dp}(r) = \epsilon$  if  $r < (\sigma_d + \sigma_p)/2$  and zero otherwise, and we will restrict ourselves to  $\beta\epsilon = 0$  below. Number densities for species  $i = c, p, d$  are  $\rho_i = N_i/V$ ; packing fractions are denoted by

$\eta_i = \pi \sigma_i^3 \rho_i / 6$ . In general,  $s = \sigma_d / \sigma_c$  is a further control parameter for the ternary mixture; for the present purpose we are interested only in  $s \rightarrow \infty$ , such that we can expand the (Helmholtz) free energy  $F$  for the ternary mixture to linear order in the surface of the dummy particles,  $\pi \sigma_d^2 \rho_d V$ , as

$$F/V = (1 - \eta_d) f(\eta_c, \eta_p, q) + \pi \sigma_d^2 \rho_d \gamma_{\text{wf}}(\eta_c, \eta_p, q), \quad (1)$$

where  $f$  is the free energy per volume of the binary colloid–polymer mixture, and the factor  $1 - \eta_d$  corrects for the finite volume that the dummies occupy. Once  $F$  (and  $f = \lim_{\rho_d \rightarrow 0} F/V$ ) is known, equation (1) provides a means to determine  $\gamma_{\text{wf}}$ .<sup>4</sup>

In our first case we use  $F$  as obtained from free volume theory [20], where the dummy is a hard sphere, to obtain the hard wall–fluid interface tension of the AO model ( $\beta\epsilon = 0$ ),

$$\beta \gamma_{\text{wf}} = \beta \gamma_{\text{hs}} + \rho_p \frac{\sigma_p}{2} [1 + (1 + 3q + q^2)\tau + (3q + 4q^2)\tau^2 + 3q^2\tau^3], \quad (2)$$

where  $\tau = \eta_c / (1 - \eta_c)$  and  $\beta \sigma_c^2 \gamma_{\text{hs}} = 3\eta_c(2 + \eta_c) / [2\pi(1 - \eta_c)^2]$  is the interface tension of pure hard spheres and a hard wall according to scaled particle theory [27]. Clearly, our result for the AO model recovers  $\gamma_{\text{hs}}$  for  $\eta_p = 0$ . In the case  $\eta_c = 0$ , equation (2) yields  $\beta \gamma_{\text{wf}} = \sigma_p \rho_p / 2$ , which is exact for the ideal gas of polymers at the hard wall. Different conventions for  $\gamma_{\text{wf}}$  exist; including the work to displace the particle centres over a distance of one radius (as for example in [27]) yields the tension  $\gamma_{\text{wf}} - \sum_{i=c,p} P \sigma_i / 2$ , where the bulk pressure is  $\beta P = \beta P_{\text{hs}} + \rho_p(1 - \rho_c \alpha' / \alpha)$ , with the hard sphere contribution  $\beta P_{\text{hs}} = 6\eta_c(1 + \eta_c + \eta_c^2) / [\pi \sigma_c^3(1 - \eta_c)^3]$ , and the term involving the free volume fraction  $\alpha$  [20] and  $\alpha' = \partial \alpha / \partial \rho_c$  is  $-\rho_c \alpha' / \alpha = (1 + 3q + 3q^2 + q^3)\tau + (3q + 12q^2 + 7q^3)\tau^2 + (9q^2 + 15q^3)\tau^3 + 9q^3\tau^4$ . It is interesting to note that  $\gamma_{\text{wf}}$  given through (2) shares linearity in  $\rho_p$  with the bulk excess (over ideal) free energy,  $F_{\text{exc}}$ , for the AO model from free-volume theory [20]. Recall that  $F_{\text{exc}}$  is related to the SPT result for the excess free energy of binary hard spheres through linearization of the latter with respect to the density of one of the components (becoming the polymer); see [13] for further discussion and the relation to DFT. Remarkably, the same property holds for the tension. Linearizing the result of  $\gamma_{\text{wf}}$  for binary hard sphere mixtures (given in equation (3.9) of [29] and reformulated in Rosenfeld form in equation (26) of [32]) in one of the packing fractions yields equation (2). For the step-function interaction between polymers, a free energy for the ternary mixture (where the dummies act like colloids) is given using the framework of [23]. We obtain for the hard wall-tension  $\gamma_{\text{wf}} + \Delta \gamma_{\text{wf}}$ , where  $\gamma_{\text{wf}}$  is given in (2) and up to cubic order<sup>5</sup> in  $\beta\epsilon$ :

$$\begin{aligned} \Delta \gamma_{\text{wf}} \sigma_c^2 &= \frac{3\eta_p^2}{2\pi q^2} \left[ \beta\epsilon - \frac{(\beta\epsilon)^2}{2} \right] (1 + \tau)^2 (5 + 12q\tau + 2q^2\tau + 9q^2\tau^2) + \frac{\eta_p^2 (\beta\epsilon)^3}{4\pi q^2} (1 + \tau)^2 \\ &\times [5 + 12q\tau + 2q^2\tau + 9q^2\tau^2 + 12\eta_p(1 + \tau)(4 + 9q\tau + q^2\tau + 6q^2\tau^2)]. \end{aligned} \quad (3)$$

In the second case, we apply the same procedure as above to a ternary AO model with a dummy *polymer* species (with  $\beta\epsilon = 0$ ), in order to obtain  $\gamma_{\text{wf}}$  of a wall that acts as a big polymer, i.e. it is penetrable to the polymers but impenetrable to the colloids. Carrying out the analysis reveals that in this case simply  $\gamma_{\text{wf}} = \gamma_{\text{hs}}$ , being *independent* of the polymer density.

As benchmarks we have carried out numerical DFT calculations using the theory of [13], which is specifically tailored for the AO model. The planar walls are described by external

<sup>4</sup> Note that similar to the hard sphere case [32], the geometrical DFT for the binary colloid–polymer mixture [13, 23] yields  $\gamma_{\text{wf}} = \partial \Phi / \partial n_2^{(i)}$  as the tension of a planar wall that behaves like species  $i$ , where  $\Phi$  is the free energy density and  $n_2^{(i)}$  is the surface weighted density of species  $i$ .

<sup>5</sup> Nonperturbative results can be obtained numerically from constructing the bulk free energy from numerical solution of the 0d problem; see [23].

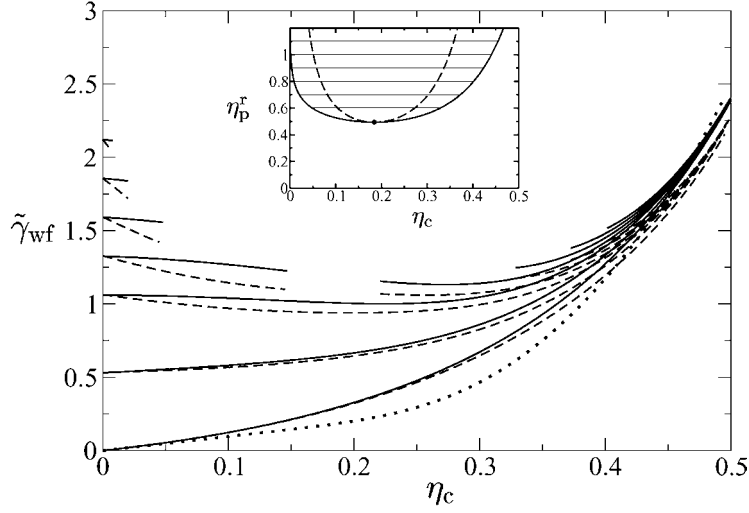


**Figure 1.** The hard wall–fluid interface tension  $\tilde{\gamma}_{wf} = \beta\sigma_c^2\gamma_{wf}$  of the AO model for size ratio  $q = \sigma_p/\sigma_c = 0.6$  as a function of the colloid packing fraction  $\eta_c$  and for increasing polymer reservoir packing fractions  $\eta_p^r = 0, 0.2, 0.4, 0.5, 0.6, 0.7, 0.8$  (from bottom to top). The results from SPT (full curves) are compared to those of numerical DFT calculations (dashed curves). The gap in the top four curves corresponds to fluid phase coexistence. Also shown is the DFT result for the polymer-coated wall for  $\eta_p^r = 0.4$  (dotted curve); the corresponding SPT result is equal to  $\gamma_{hs}$  (lowest full curve). The inset shows the fluid part of the phase diagram for  $q = 0.6$  as a function of  $\eta_c$  and  $\eta_p^r$ ; indicated are the binodal (thick curve), spinodal (dotted curve), critical point and (horizontal) tielines connecting coexisting states.

potentials  $u_i(z)$  acting on species  $i = c, p$ , where  $z$  is the distance from the wall, and  $u_i(z) = \lim_{\sigma_d \rightarrow \infty} u_{di}(z - \sigma_d)$ . Inhomogeneous colloid and polymer density profiles as a function of  $z$  are obtained through iteration. The wall tension  $\gamma_{wf}$  is calculated via evaluating the grand potential functional for these solutions and subtracting the bulk contribution  $-PV$  where  $V$  is the volume with  $z > 0$  and also subtracting  $-\beta\rho_p V_-$  in the case of the polymer-coated wall, where  $V_-$  is the volume with  $z < 0$ ; see for example [15] for more details.

We first consider the case of the hard wall; see figure 1 for  $\gamma_{wf}$  as a function of  $\eta_c$  for different values of  $\eta_p^r$ , being the packing fraction of polymers in a reservoir of pure polymer that is in chemical equilibrium with the system. In the pure hard sphere case,  $\eta_p^r = 0$ , the SPT result, (2), is equal to the accurate hard sphere result [27], whereas the DFT reduces to the also accurate Rosenfeld hard sphere functional. Both agree well [32], the DFT giving slightly smaller values for  $\gamma_{wf}$  for high  $\eta_c$ . Increasing  $\eta_p^r$  at constant  $\eta_c$  significantly increases  $\gamma_{wf}$ . Recall that for  $\eta_c = 0$  equation (2) becomes exact, and indeed both approaches give this limiting value. The behaviour for small  $\eta_c > 0$  is qualitatively correct in the SPT treatment, but quantitatively significantly stronger in DFT. The latter takes the depletion attraction between wall and colloid mediated by the polymer [34] correctly into account, which we expect not to be the case in the SPT. Increasing  $\eta_c$  at constant  $\eta_p^r$  reduces  $\eta_p$  in the system, and the hard sphere result is approached smoothly.  $\gamma_{wf}$  is non-monotonic and goes through a minimum located at an intermediate value of  $\eta_c$ , provided  $\eta_p^r$  is large enough, in the SPT  $\eta_p^r > 1/(2+q)$  ( $=0.384$  for  $q = 0.6$ ). The gap for results above the critical point,  $\eta_p^r > \eta_p^{r,crit} \approx 0.494$ , indicates fluid–fluid phase coexistence. No apparent anomaly occurs in the analytic result either at the binodal or at the spinodal. Generally the agreement between results from SPT and DFT is good. In the case of the polymer-coated wall the SPT result for  $\gamma_{wf}$  is for all  $\eta_p^r$  identical to  $\gamma_{hs}$ , hence the polymers are predicted to have *no* effect on the interface tension. To test this

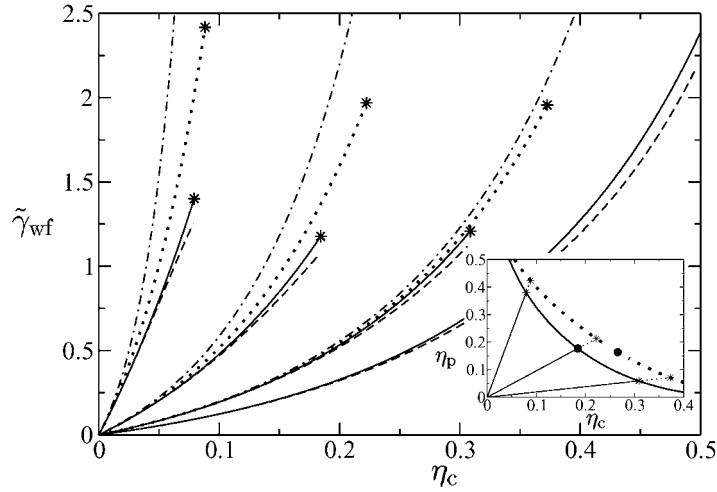


**Figure 2.** The hard wall–fluid interface tension  $\tilde{\gamma}_{\text{wf}} = \beta\sigma_c^2\gamma_{\text{wf}}$  of the AO model for size ratio  $q = 0.6$  as a function of  $\eta_c$  along dilution lines,  $\eta_p = \kappa\eta_c$ , for  $\kappa/\kappa_{\text{crit}} = 0, 0.2, 1, 5$  (right to left), where  $\kappa_{\text{crit}} = \eta_p^{\text{crit}}/\eta_c^{\text{crit}} = 0.9599$  is the slope of the dilution line through the critical point. Compared are results from SPT (full curves) and DFT calculations (dashed curves) for statepoints in the single-phase region and ending at the binodal (indicated by stars). Also shown are results from SPT for the case of interacting polymers for  $\beta\epsilon = 0.5$  (dotted curves) and for binary hard spheres (chain curves) for the same densities and size ratio. The inset shows the phase diagram as a function of  $\eta_c$  and  $\eta_p$  with the binodals for the AO model (thick full curve) and for the interacting-polymer case ( $q = 0.6; \beta\epsilon = 0.5$ ) (dotted curves), as well as the corresponding critical points (filled dots) and dilution lines (straight lines).

we compare for one fugacity,  $\eta_p^f = 0.4$ , with the DFT result for  $\gamma_{\text{wf}}$ , which takes the polymers explicitly into account. Indeed, it deviates little from the hard-sphere DFT result, mainly for intermediate values of  $\eta_c$ .

We next follow dilution lines, which are experimentally convenient paths in the phase diagram obtained by keeping the total colloid and polymer mass (inside a cuvette) constant; adding solvent then decreases both  $\eta_c$  and  $\eta_p$  while keeping the ratio  $\kappa = \eta_p/\eta_c = \text{constant}$ . In figure 2  $\gamma_{\text{wf}}$  is plotted for different values of  $\kappa$  as a function of  $\eta_c$  in the one-phase region. The hard sphere result for  $\kappa = 0$  serves as a reference. Following dilution lines at  $\kappa > 0$  leads to a much stronger increase of  $\gamma_{\text{wf}}$  with  $\eta_c$ , clearly an effect of the added polymer. The increase becomes stronger for steeper dilution lines, i.e. upon increasing  $\kappa$ . The comparison between SPT and DFT results is somewhat better than in figure 1 (where more extreme statepoints were considered). It is interesting to compare these results with those for two other models. The first is the binary hard sphere mixture (obtained by replacing the polymers with hard spheres) of size ratio  $q = 0.6$  and the same packing fractions; see figure 2 for the results. The SPT result for the binary hard sphere mixture [29], known to deviate only little from explicit DFT calculations [32], indicates significantly larger tension than the AO model at the same statepoint, clearly due to stronger packing effects. Secondly, we plot the result for polymers interacting with a stepfunction pair potential, equations (2) and (3). This model possesses an additional energy scale that governs the strength of the polymer–polymer interaction. Already for the very moderate value of  $\beta\epsilon = 0.5$  (where we expect the cubic order expression given in (3) to be accurate) we find a significant increase of  $\gamma_{\text{wf}}$  over the ideal (AO) case. Moreover, along each dilution line larger values of  $\eta_c$  can be reached inside the one-phase region, as the binodal for the case of non-ideal polymers is shifted towards higher  $\eta_c$  and  $\eta_p$ , hence demixing is suppressed (see the inset in figure 2 and [23] for further background).

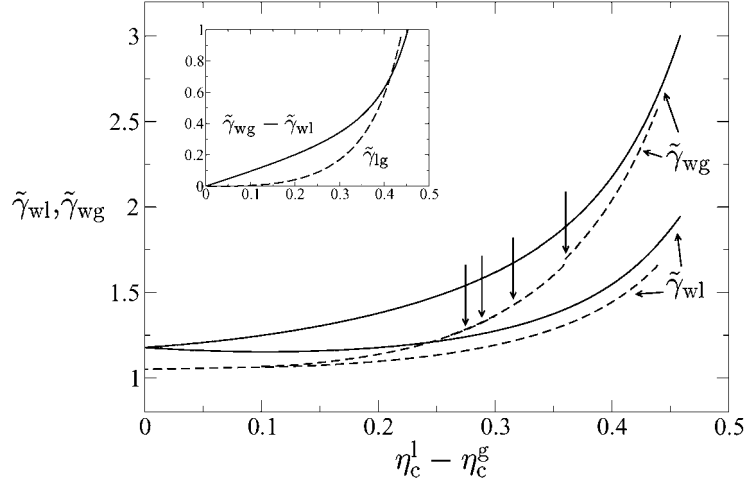


**Figure 3.** Hard wall–fluid interface tensions of the AO model for size ratio  $q = 0.6$  at fluid–fluid coexistence as a function of the difference in coexisting colloid packing fractions,  $\eta_c^l - \eta_c^g$ . Shown are the results from SPT (full curves) and from numerical DFT calculations (dashed curves) for  $\tilde{\gamma}_{wg} = \beta\sigma_c^2\gamma_{wg}$  and  $\tilde{\gamma}_{wl} = \beta\sigma_c^2\gamma_{wl}$ . Marked are the positions of the first, second and third layering transition and the wetting transition (vertical arrows, from right to left, taken from [14]) that appear on the gas branch of the binodal [14]. The DFT result for  $\tilde{\gamma}_{wg}$  in the complete wetting regime (between the origin and the leftmost arrow) is obtained as  $\tilde{\gamma}_{wl} + \tilde{\gamma}_{lg}$ . Note the jump in the DFT result for  $\tilde{\gamma}_{wg}$  at the first layering transition (rightmost arrow). The inset shows the analytic result for the difference  $\tilde{\gamma}_{wg} - \tilde{\gamma}_{wl}$  and the DFT result for the interface tension of the free liquid–gas interface,  $\tilde{\gamma}_{lg} = \beta\sigma_c^2\gamma_{wl}$  [14]; the crossing point indicates the result for the wetting transition within this treatment.

At bulk fluid–fluid coexistence a dense colloidal liquid with packing fractions  $\eta_c^l$  and  $\eta_p^l$  coexists with a dilute colloidal gas with packing fractions  $\eta_c^g$  and  $\eta_p^g$ . Evaluating the respective expressions for the wall fluid tension yields  $\gamma_{wg} = \gamma_{wf}(\eta_c^g, \eta_p^g)$  and  $\gamma_{wl} = \gamma_{wf}(\eta_c^l, \eta_p^l)$ ; see figure 3 for results for the AO model at a hard wall obtained from equation (2). The agreement with the results from DFT on the liquid side is again very good, but on the gas side deviations are larger due to crowding of colloids at the wall; any layering transitions [14] are not captured by the SPT. At the first layering transition [14, 15] we observe a kink in the DFT result for  $\gamma_{wg}$ . We expect the second and third layering transitions (with smaller jumps in the adsorption) to have similar anomalies, but have not been able to resolve them with the current numerical accuracy. Also the precise location of the transition from partial to complete wetting, where  $\gamma_{lg} = \gamma_{wg} - \gamma_{wl}$ , is not observable in this way. Comparing our SPT result for  $\gamma_{wg} - \gamma_{wl}$  with the DFT result for  $\gamma_{lg}$  [14], we find that close to the critical point  $\gamma_{wg} - \gamma_{wl} > \gamma_{lg}$ , indicating complete wetting, and further away from the critical point  $\gamma_{wg} - \gamma_{wl} < \gamma_{lg}$ , indicating partial wetting. Despite the simplicity of the SPT, this is qualitatively in accordance with full DFT calculations (analysing the behaviour of the inhomogeneous colloid density profile at the wall) [14, 15]. The location of the wetting transition obtained by setting  $\gamma_{lg} = \gamma_{wg} - \gamma_{wl}$ , is  $\eta_c^l - \eta_c^g = 0.41$ ,  $\eta_p^r = 0.87$ , whereas the DFT result is  $\eta_c^l - \eta_c^g = 0.276$ ,  $\eta_p^r = 0.596$  [14, 15].

Carrying out a similar analysis for the case of the polymer-coated wall (see figure 4) reveals a larger discrepancy between the SPT and DFT results, especially on the liquid side of the binodal. The SPT result for  $\gamma_{wl} - \gamma_{wg}$  does *not* cross  $\gamma_{lg}$  from DFT, indicating complete drying everywhere on the liquid branch of the binodal. Indeed drying has been observed experimentally at a polymer-coated substrate [8]. It turns out that the DFT results for  $\gamma_{wg} + \gamma_{lg}$  and  $\gamma_{wl}$  (not shown in figure 4) are practically equal on the scale of the plot. The colloid

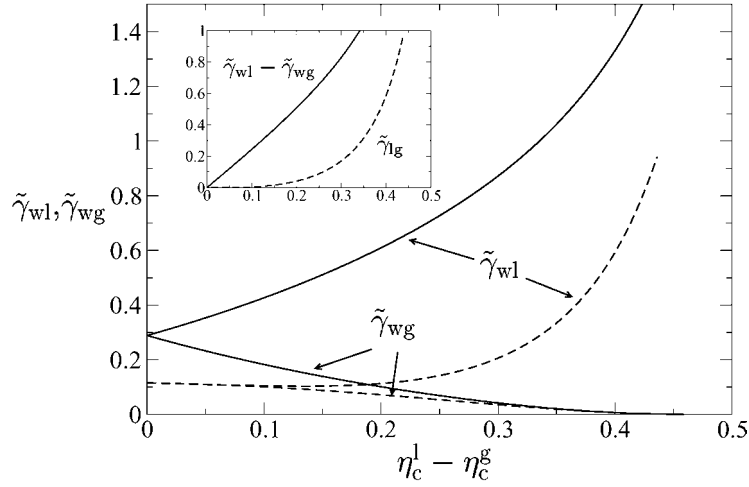


**Figure 4.** The same as figure 3 but for the polymer-coated wall. Note the different vertical scale compared to figure 3. Within the DFT we obtain  $\tilde{\gamma}_{wl}$  as  $\tilde{\gamma}_{wl} = \tilde{\gamma}_{wg} + \tilde{\gamma}_{lg}$ . The inset shows that  $\tilde{\gamma}_{wl} - \tilde{\gamma}_{wg} > \tilde{\gamma}_{lg}$ , hence complete drying on the liquid branch of the binodal, compatible with results from full DFT calculations.

density profiles show a clear layer of gas density close to the wall (which is not treated within the SPT). For one statepoint,  $\eta_p^r = 1$ , far away from the critical point, we have checked within the DFT that the adsorption  $\Gamma_c = \int_0^\infty dz (\rho_c(z) - \rho_c(\infty)) \propto \ln(\eta_c/\eta_c^1 - 1)$  over more than two decades,  $10^{-4} < \eta_c/\eta_c^1 - 1 < 10^{-2}$ , indicating complete drying. The current binary mixture adsorbed at a wall that does not generate an effective depletion interaction is closely related to simple fluids at a hard wall, where complete drying is found everywhere on the liquid branch of the binodal [35].

In conclusion, we have derived analytical expressions for the wall tension of a colloid–polymer mixture using a scaled particle approach. Both the Asakura–Oosawa model near a hard and a polymer-coated wall (the latter being penetrable for the polymers) as well as the case of interacting polymers at a hard wall are considered. Results are tested against explicit DFT calculations and good overall agreement is found. Applied to the fluid demixing binodal, our data confirm the wetting transition at the hard wall [14, 15]. Wetting at a hard wall was observed experimentally [7–9], and also a transition was claimed [8, 9]. The previously found layering transition [14, 15] manifests itself as a tiny kink in the interfacial tension. We predict complete drying near a polymer-coated wall; this was also reported in experiments [9]. Future work could be devoted to exploring the interfacial tensions by direct computer simulation via integrating the anisotropy of the pressure tensor [36], by thermodynamic integration [31] or, possibly, by using grand-canonical configurational-bias Monte Carlo [19] in order to test our predictions. It would also be interesting to study patterned surfaces [37] and structured walls which for example drastically influence the flow through microfluidic devices [38].

MS thanks M Dijkstra, A Fortini and D G A L Aarts for inspiring discussions and R Evans for very useful correspondence. A A Louis is thanked for informing us about his unpublished work. This work is financially supported by the SFB-TR6 ‘Physics of colloidal dispersions in external fields’ of the *Deutsche Forschungsgemeinschaft* (DFG). The work of MS is part of the research program of the *Stichting voor Fundamenteel Onderzoek der Materie* (FOM), that is financially supported by the *Nederlandse Organisatie voor Wetenschappelijk Onderzoek* (NWO).



## References

- [1] Poon W C K 2002 *J. Phys.: Condens. Matter* **14** R859
- [2] Pospiech D *et al* 2003 *Surf. Coat. Int.* **B 86** 43
- [3] Vliegthart G A and Lekkerkerker H N W 1997 *Prog. Coll. Polym. Sci.* **105** 27
- [4] de Hoog E H A and Lekkerkerker H N W 1999 *J. Phys. Chem. B* **103** 5274
- [5] Chen B-H, Payandeh B and Robert M 2000 *Phys. Rev. E* **62** 2369  
Chen B-H, Payandeh B and Robert M 2001 *Phys. Rev. E* **64** 042401
- [6] Aarts D G A L, van der Wiel J H and Lekkerkerker H N W 2003 *J. Phys.: Condens. Matter* **15** S245
- [7] Aarts D G A L and Lekkerkerker H N W 2003 private communication
- [8] Wijting W K, Besseling N A M and Cohen Stuart M A 2003 *Phys. Rev. Lett.* **90** 196101
- [9] Wijting W K, Besseling N A M and Cohen Stuart M A 2003 *J. Phys. Chem. B* **107** 10565
- [10] Asakura S and Oosawa F 1954 *J. Chem. Phys.* **22** 1255  
Asakura S and Oosawa F 1958 *J. Polym. Sci.* **33** 183
- [11] Vrij A 1976 *Pure Appl. Chem.* **48** 471
- [12] Brader J M and Evans R 2000 *Europhys. Lett.* **49** 678
- [13] Schmidt M, Löwen H, Brader J M and Evans R 2000 *Phys. Rev. Lett.* **85** 1934  
Schmidt M, Löwen H, Brader J M and Evans R 2002 *J. Phys.: Condens. Matter* **14** 9353
- [14] Brader J M, Evans R, Schmidt M and Löwen H 2002 *J. Phys.: Condens. Matter* **14** L1
- [15] Brader J M, Evans R and Schmidt M 2003 *Mol. Phys.* at press
- [16] Schmidt M, Fortini A and Dijkstra M 2003 *J. Phys.: Condens. Matter* **15** 53411
- [17] Dijkstra M and van Roij R 2002 *Phys. Rev. Lett.* **89** 208303
- [18] Bolhuis P G, Louis A A and Hansen J-P 2002 *Phys. Rev. Lett.* **89** 128302
- [19] Vink R L C and Horbach J 2003 *Preprint cond-mat/0310404*
- [20] Lekkerkerker H N W, Poon W C K, Pusey P N, Stroobants A and Warren P B 1992 *Europhys. Lett.* **20** 559
- [21] Aarts D G A L, Dullens R P A, Lekkerkerker H N W, Bonn D and van Roij R 2003 *J. Chem. Phys.* at press
- [22] Moncho-Jordá A, Rotenberg B and Louis A A 2003 *Preprint cond-mat/0309248*
- [23] Schmidt M, Denton A R and Brader J M 2003 *J. Chem. Phys.* **118** 1541
- [24] Dietrich S 1988 Wetting phenomena *Phase Transitions and Critical Phenomena* ed C Domb and J L Lebowitz (London: Academic) p 1
- [25] Louis A A, Bolhuis P G, Meijer E J and Hansen J-P 2002 *J. Chem. Phys.* **116** 10547
- [26] Reiss H, Frisch H L and Lebowitz J L 1959 *J. Chem. Phys.* **31** 369
- [27] Reiss H, Frisch H L, Helfand E and Lebowitz J L 1960 *J. Chem. Phys.* **32** 119
- [28] Lebowitz J L and Rowlinson J S 1964 *J. Chem. Phys.* **41** 133
- [29] Lebowitz J L, Helfand E and Praestgaard E 1965 *J. Chem. Phys.* **43** 774
- [30] Henderson J R 2002 *J. Chem. Phys.* **116** 5039
- [31] Heni M and Löwen H 1999 *Phys. Rev. E* **60** 7057
- [32] Roth R and Dietrich S 2000 *Phys. Rev. E* **62** 6926
- [33] Tenne R and Bergmann E 1978 *Phys. Rev. A* **17** 2036
- [34] Brader J M, Dijkstra M and Evans R 2001 *Phys. Rev. E* **63** 041405
- [35] Parry A O and Evans R 1988 *Mol. Phys.* **65** 45  
Parry A O and Evans R 1993 *Mol. Phys.* **78** 1527
- [36] Walton J P R B, Tildesley D J, Rowlinson J S and Henderson J R 1983 *Mol. Phys.* **48** 1357
- [37] Henderson J R 2003 *Mol. Phys.* **101** 397
- [38] Drazer G, Koplik J, Acrivos A and Khusid B 2002 *Phys. Rev. Lett.* **89** 244501